

**The Henryk Niewodniczański  
INSTITUTE OF NUCLEAR PHYSICS  
Polish Academy of Sciences**  
ul. Radzikowskiego, 31-342 Kraków, Poland

[www.ifj.edu.pl/publ/reports/2010/](http://www.ifj.edu.pl/publ/reports/2010/)

Kraków, March 2010

## **Report No. 2038/AP**

### **Spectrometric properties of the CVD diamond detector for measurement of the ‘lost alpha particles’**

*Iwona Wodniak<sup>1</sup>, Jan Dankowski, Krzysztof Drozdowicz, Barbara Gabańska,  
Andrzej Igielski, Arkadiusz Kurowski, Barbara Marczewska, Tomasz Nowak*

<sup>1</sup> Interdisciplinary PhD Studies, AGH Univ. of Science and Technology, Kraków, Poland

The research has been supported by the EFDA (European Fusion Development Agreement) WP08-09-DIAG-01-02 Task Agreement “Escaping Fast Alpha Diagnostics” and the Association EURATOM–IPPLM (Poland).

#### **Abstract**

Measurement of energy of the ‘escaping alpha particles’ from the thermonuclear reaction in the tokamak is important to get information on the energetic balance in future thermonuclear reactors producing electrical energy. Detectors will work in a harsh environment (high fluxes of particles, high temperature). Synthetic (CVD) diamond can be used in this case as a semiconductor detector. Tests with such a detector are described. Energy calibration has been carried out with a triple alpha particle isotopic source,  $^{239}\text{Pu}$ ,  $^{241}\text{Am}$ ,  $^{244}\text{Cm}$  (PAC), with the  $\alpha$  energy peaks at ca. 5.2, 5.5 and 5.8 MeV. A very good energy resolution has been obtained, comparable with the resolution of the classic silicon detector. Energy response has been also investigated with the use of monoenergetic alpha particle beams (0.4 to 2 MeV) from the Van de Graaf accelerator. The amplitude linearity of the signal is very good, including besides results of measurements with the PAC source.

## 1. Introduction

In tokamak devices it is feasible to produce and maintain high temperature plasma which is controlled by magnetic and electric field. Plasma diagnostic is the biggest task facing the scientists. Knowledge of the most important plasma parameters such as temperature, density, radiation loss, is essential to understanding of the behavior of high temperature plasma. Plasma diagnostic methods are usually innovative in nature and always refer to physical processes which bring information on individual parameters. The conditions prevailing within the torus are not compatible with conventional diagnostic methods, hence the need to seek new solutions and materials that will be resistant during tokamak operation. Measurement of escaping alpha rates to the first wall is of importance in planning tokamak fusion reactors [1], [2]. In the International Thermonuclear Experimental Reactor (ITER) alpha particles will be produced in the thermonuclear reaction between light atomic nuclei, deuterium and tritium, fusing to form helium and a neutron [3]:



The kinetic energy  $E$  is shared 14.1 MeV and 3.5 MeV between the neutron and the helium ( ${}^4He$ ) nucleus. The  $\alpha$  particles produced by the fusion reactors help to maintain the plasma at a right temperature for the ongoing fusion, and also heat the incoming fuel. The lost  $\alpha$  effect should be concerned for few reasons. Losses of  $\alpha$  particles from plasma could extinguish the burn and might melting the first wall [3], [4]. Therefore, it is important to know energy of the escaping  $\alpha$  particles. Semiconductor detectors usually can be used for the spectrometric  $\alpha$  measurements; silicon detectors, for example. However, silicon can be easily damaged in high flux and high temperature environment. Diamond detectors have strong advantages for use in applications for  $\alpha$  particle detection in the tokamak environment. In this case diamond is a better material for detecting high energy particles like  $\alpha$  particles, neutrons, electrons and other.

Diamond has some of the most extreme physical properties of any materials and such properties as its radiation and corrosion resistance, large band gap, high electron and hole mobility make it an attractive semiconductor detector used of spectroscopy in real time measurements. Diamonds, as detectors of high energy  $\alpha$  particles, within the operating reactor chamber, in special diagnostics ports, prove more efficient and resistant than the silicon or germanium detectors [5].

Diamond detectors have extended history. In the 1920's diamond were used in photoconductive ultraviolet detectors by Gudden and Pohl and ionizing radiation detectors were produced in the 1940's by Hofstadter. Interactions of  $\alpha$  particles and high energy

electrons with diamond were studied through the 1950's and 60's. However, these detectors found restricted usage due to limitations of natural diamonds. Specifically, the restrictions of this type are small size and uncontrolled material characteristics. Current technologies allow grow diamond crystals [6]. Quality and size of Chemical Vapor Deposition (CVD) diamonds created new opportunities for fabrication and application of diamond detectors.

The use of diamond as a material for the construction of detectors for high temperature plasma diagnostics provide information on the profile of the formation of  $\alpha$  particles as well as on the efficiency of plasma heating. The choice of diamond material is essential because of its good parameters like radiation hardness, fast response and high energy resolution. Diamond has many excellent parameters which make it an attractive material for radiation detectors in most hard conditions. The large band gap (5.5 eV), radiation hardness, optical transparency, large saturated currier velocity, high breakdown ( $10^7$  V/cm) and high resistivity ( $10^{11}$   $\Omega$ cm) make it an ideal material for many applications [6], [7]. These parameters and many others have shown that diamond appears as good as silicon. Any radiation that generates free carriers in diamond can be detected, including UV, X-ray and gamma ray although the low atomic number gives low sensitivity for these types of radiation [8]. The transport of the generated charge proceeds independently of the exciting radiation type. Drift of free charges, electrons and holes, generates the electrical current in the external circuit. The large mobility of electrons and holes is a key property of the diamond detector. This high mobility is a partial consequence of the high Debye temperature and inelasticity of the material. In a low electric filed and the temperature about 20 °C, the electron mobility is about  $1800\text{ cm}^2\text{V/s}$  and the hole mobility is  $1200\text{ cm}^2\text{V/s}$  [10]. At higher temperatures mechanism of phonon scattering dominates and is scaling as  $T^{-3/2}$ . In low temperatures this effects is invisible and ionized impurity scattering can dominate [9].

A project of European Fusion Development Agreement (EFDA) has been undertaken to develop a method for detection of the escaping  $\alpha$  particles. One of the tasks is devoted to research on possible application of the diamond detectors. In the present study, a possibility of spectrometric measurements of the escaping  $\alpha$  particles with CVD diamond detectors has been tested.

## 2. Calibration of the diamond and silicon detectors

The diamond and silicon detectors have been used in the experiment. The diamond detector<sup>1</sup> is a high purity single crystal plate that has a thickness 0.05 (+0.01, -0.02) mm, size of 2.5 mm  $\times$  2.5 mm ( $\pm 0.01$  mm) and gold contacts of the thickness of 20 nm. The active diameter

---

<sup>1</sup> Diamond Detector Ltd.

of the diamond detector is 1.9 mm and the diameter of the detector together with housing is 27 mm. The silicon detector is a crystal plate that has a thickness 0.5 mm. The diameter of the detector without housing is 10 mm, the diameter of the detector housing is 20 mm.

The energy calibration of the diamond and silicon detectors has been performed in a vacuum chamber. The radioactive source  $^{239}\text{Pu}$   $^{241}\text{Am}$   $^{244}\text{Cm}$  (PAC) has been put on the surface of the detector during the calibration measurements. These calibrations have been done to compare results of the measurements with the diamond and silicon detectors. The PAC source emits  $\alpha$  particles and their energies [11] are presented in Table 1.

**Table 1.** Energy of  $\alpha$  particles emitted by the PAC source.

$^{239}\text{Pu}$		$^{241}\text{Am}$		$^{244}\text{Cm}$	
$E_\alpha$ (keV)	$P_\alpha$ (%)	$E_\alpha$ (keV)	$P_\alpha$ (%)	$E_\alpha$ (keV)	$P_\alpha$ (%)
5156.65	70.76	5485.68	84.4	5804.86	76.6
5143.9	17.16	5442.98	13.1	5762.74	23.4
5105.89	11.92	5388.40	1.65		

$E_\alpha$  – energy of  $\alpha$  particles  
 $P_\alpha$  – fraction of  $\alpha$  particles that have energy  $E_\alpha$ .

The energy resolution of the diamond detector has been evaluated using the detection line consisting of the diamond detector SO153 with the SMA connector to the charge preamplifier ORTEC 142A, the spectroscopy amplifier ORTEC 672, the multichannel analyzer ORTEC 927 and a computer. A schematic block diagram of the detection line is presented in Fig. 1.

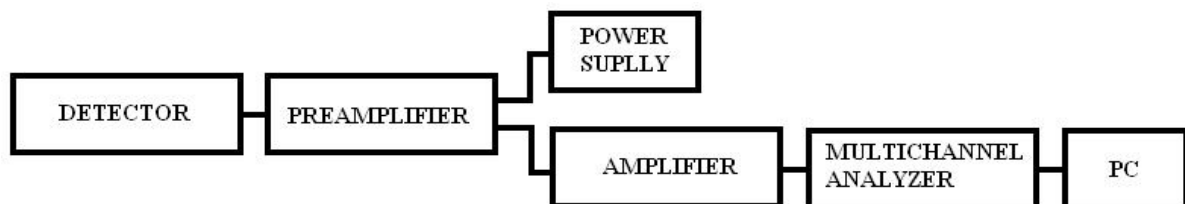


**Fig. 1.** Block diagram of the detection line.

Parameters of the detection line have been following: power supply –50 V, amplification  $10 \times 100$ , the maximum number of channels of the multichannel analyzer is 8200. The diamond detector has always been operated and stored at the room temperature. Parameters of

the detection line for the silicon detector have been following: power supply 126 V, amplification  $4 \times 100$ . The spectrum emitted from the PAC source has been acquired with the silicon detector using electronics of the same type as for the diamond detector. The time of data collection has been equal 1800 s.

The  $\alpha$  spectra acquired using the diamond and silicon detectors are shown in Fig. 2. The PAC source emits  $\alpha$  particles with three main energies, therefore three corresponding peaks are clearly visible in the spectrum. There are other small peaks that appear at the left hand side of the main peaks due to small contributions of  $\alpha$  particles emitted by the PAC source with smaller energies.

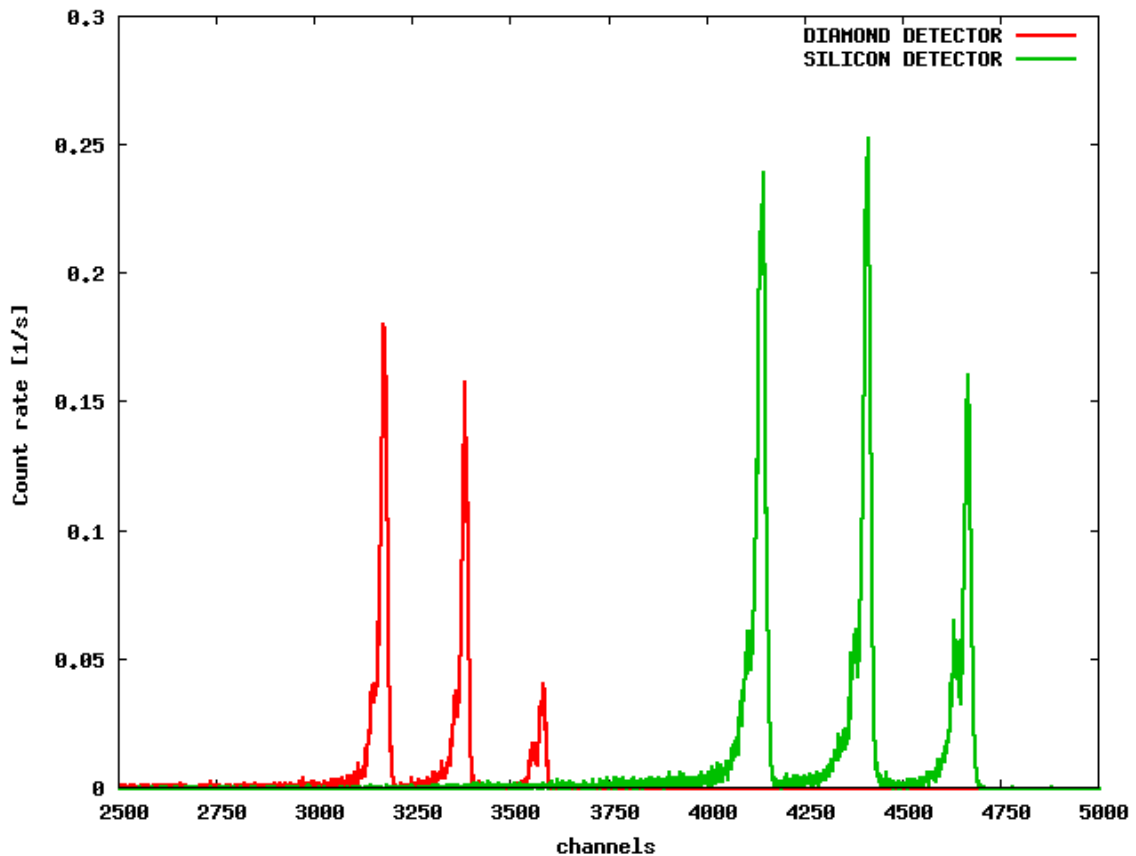


**Fig. 2.** Spectra of the PAC source recorded with the diamond and silicon detectors.

On the basis of the numbers of channels and of corresponding energies of  $\alpha$  particles the calibration lines have been obtained for the diamond and silicon detectors. The calibration lines are plotted in Fig 3. A linear relation between the numbers of channels and the energy is observed. Parameters,  $a$ ,  $b$ , of the line  $y=ax+b$  are given in Table 2.

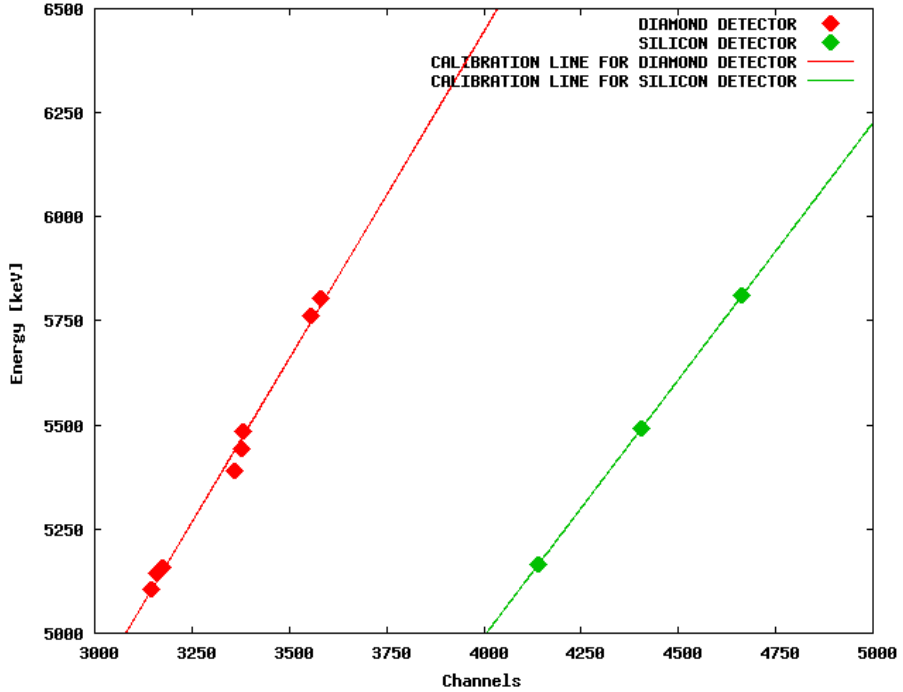


**Fig. 3.** Calibration lines for the diamond and silicon detectors.

**Table 2.** Parameters of the calibration lines  $y=ax+b$  for the detectors.

Parameter	Diamond detector	Silicon detector
$a$	1.570	1.23433
$\sigma(a)$	0.059	0.00001
$b$	163	54.895
$\sigma(b)$	198	0.023
$\sigma(a), \sigma(b)$ – standard deviations		

Using the obtained calibration lines, the peak  $\alpha$ -energies in the spectra have been determined. In this way the correctness of the calibration lines have been checked. The differences between energy of  $\alpha$  particles emitted by the PAC source and these returned energy values are small and do not exceed the half-width of the peaks. The results are listed in Table 3. The diamond detector shows as good resolution as the silicon detector.

**Table 3.** Alpha particle energies returned from the calibration lines and energy resolutions of the detectors.

$E_t$ (keV)	Diamond detector				Silicon detector			
	$E_m$ (keV)	$E_t - E_m$ (keV)	$\Delta E$ (keV)	$\Delta E/E_m$ (%)	$E_m$ (keV)	$E_t - E_m$ (keV)	$\Delta E$ (keV)	$\Delta E/E_m$ (%)
5156.65	5146.25	10.4	23.13	0.45	5166.22	-9.57	23.65	0.46
5485.68	5469.25	15.93	26.15	0.48	5495.79	-10.11	19.65	0.36
5804.86	5783.83	21.03	20.72	0.36	5813.00	-8.14	19.01	0.33

$E_t$  – energy of  $\alpha$  particles emitted by the PAC source  
 $E_m$  – determined peak energy of  $\alpha$  particles  
 $\Delta E$  – full width at half maximum of the peak

### 3. Test with the Bi+Po source

A test measurement with the radioactive source  $^{212}\text{Bi} + ^{212}\text{Po}$  has been carried out as well using both detectors. The source  $^{212}\text{Bi} + ^{212}\text{Po}$  also emits  $\alpha$  particles but with higher energies than the PAC source. Energy values of  $\alpha$  particles from the Bi+Po source [11] are presented in Table 4. The source has been put on the surface of the detectors like it was in the calibration measurements.

**Table 4.** Energy of  $\alpha$  particles emitted by the  $^{212}\text{Bi} + ^{212}\text{Po}$  source.

$^{212}\text{Bi}$		$^{212}\text{Po}$	
$E_\alpha$ (keV)	$P_\alpha$ (%)	$E_\alpha$ (keV)	$P_\alpha$ (%)
6050.92	25.1	8785.06	100

The energy spectra of the  $^{212}\text{Bi} + ^{212}\text{Po}$  source recorded with the diamond and silicon detectors are presented in Fig. 4. Values of the  $\alpha$  peak energies and the energy resolutions for the diamond and silicon detectors are collected in Table 5. It should be noticed that agreement between the measured energies and theoretical values of energy of  $\alpha$  particles emitted by the Bi+Po source points out the calibration lines to be very accurate in a wide range of energy for both detectors.

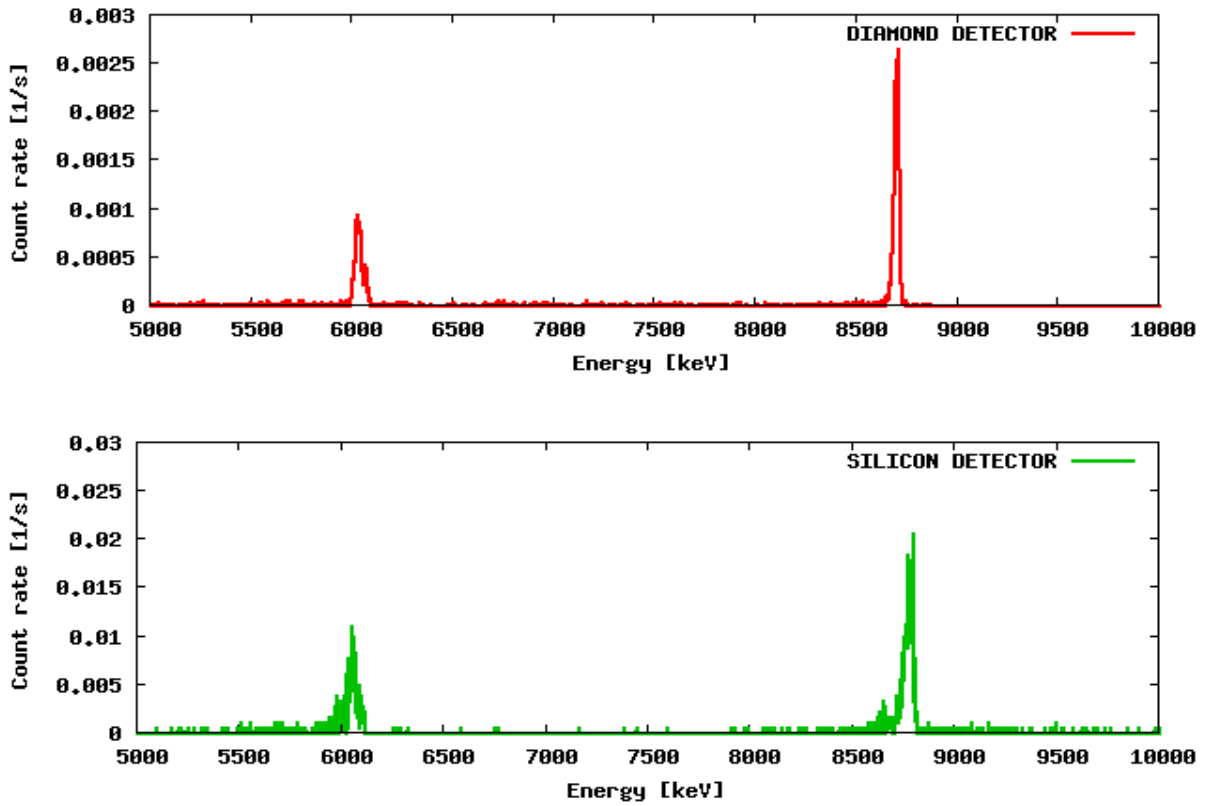


**Fig. 4.** Energy spectra of the  $^{212}\text{Bi} + ^{212}\text{Po}$  source recorded with the diamond and silicon detectors.

**Table 5.** Measured energy of  $\alpha$  particles from  $^{212}\text{Bi} + ^{212}\text{Po}$  source.

$E_t$ (keV)	Diamond detector				Silicon detector			
	$E_m$ (keV)	$E_t - E_m$ (keV)	$\Delta E$ (keV)	$\Delta E/E_m$ (%)	$E_m$ (keV)	$E_t - E_m$ (keV)	$\Delta E$ (keV)	$\Delta E/E_m$ (%)
6050.92	6022.53	28.39	29.60	0.49	6048.80	2.12	11.8	0.19
8785.06	8701.63	83.43	29.55	0.33	8792.66	-7.6	37	0.42
Symbols as in Table 3.								

#### 4. Measurements of monoenergetic ion beams

The measurements have been carried out in a laboratory of the Institute of Nuclear Studies (Swierk/Otwock, Warsaw Branch, Poland). The Van de Graaff accelerator has been used to accelerate the once-ionized helium ions ( ${}_2^4\text{He}^+$ ) to obtain finally monoenergetic beam of the  $\alpha$  particles. The beam of ions has fallen on a scattering foil held by two handles. Only the ions scattered back under the angles  $\beta$  ( $45^\circ$ ) and  $\gamma$  ( $30^\circ$ ) have been detected (Fig. 5). Again, two

detectors have been used: the diamond and silicon detectors. The first one has been placed under the  $\beta$  angle with respect to the beam of the ions. The second detector has been placed on the opposite side of the ions beam under the  $\gamma$  angle. The positions of the detectors could be changed and they could be placed along these directions nearer or further from the scattering foil. The whole arrangements have been placed in a vacuum chamber which has been connected with the accelerator through the pipe 1. Two collimators have been set within the pipe 1: the first one has had the diameter 2 mm, the second one has had the diameter 1 mm and has been placed at the distance of 170 mm from the first one. The accelerated ion beam has passed along the pipe 1 and then has been introduced into the vacuum chamber. The ions which have undergone through the foil have been collected in the Faraday's box. The electronic lines have been the same as in the calibration measurements (section 2).

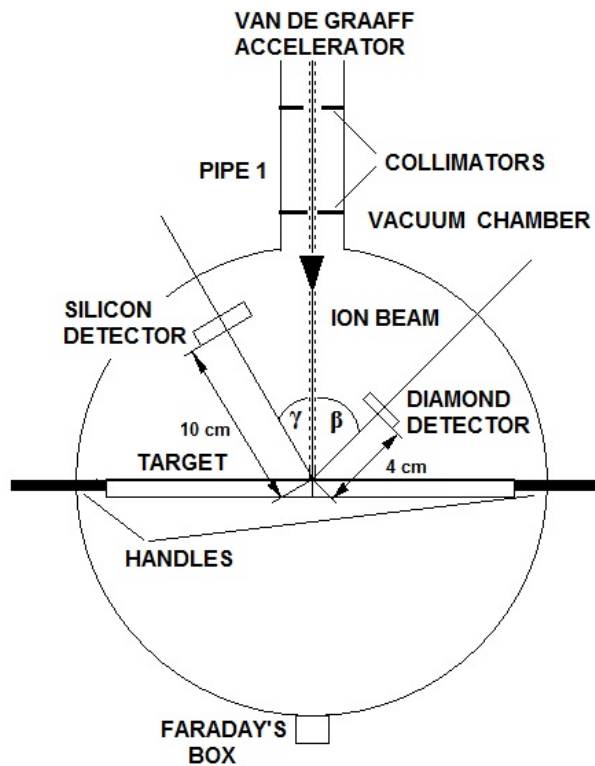


**Fig. 5.** Geometry of detection of the backscattered ions.

A thin foil of gold ( $100 \mu\text{g}/\text{cm}^2$ ) has been bombarded by the beam of helium  ${}_{2}^{4}\text{He}^{+}$  ions during the measurements. The incident ions have penetrated the foil of gold and have interacted via either inelastic collisions with electrons or elastic collisions with the atoms of gold. The incident ion of mass  $M$  and energy  $E_0$  and the gold atom of mass  $M_1$  have participated in the elastic collision.

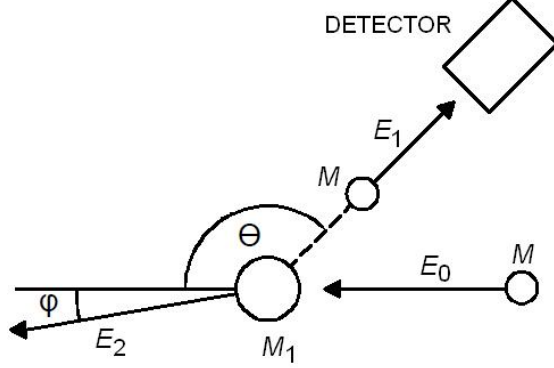


**Fig. 6.** Elastic collision between the incident ion of mass  $M$  and energy  $E_0$  with the gold atom of mass  $M_1$ .

The ion has been scattered back under the angle  $\theta$  ( $\theta = 180^\circ - \beta = 135^\circ$  or  $\theta = 180^\circ - \gamma = 150^\circ$  for the diamond and silicon detectors, respectively) and has emerged from the foil with the energy  $E_1$  while the gold atom has received the recoil energy  $E_2$ . The ratio of the ion energies before and after elastic collision is given by [12]:

$$K = \frac{E_1}{E_0} = \left[ \frac{(M_1^2 - M^2 \sin \theta)^{1/2} + M \cos \theta}{M_1 + M} \right]^2. \quad (2)$$

The incident energies  $E_0$  of the ion beam have been following: 400 keV, 1000 keV, 1500 keV and 2000 keV. Knowing the energy of the incident ions of helium and the  $\theta$  angles the energy  $E_1$  of scattered helium ions have been calculated. Equation (2) is exactly fulfilled for one-atomic layer of the gold. This calculation is not precise enough. For a better estimation of energy of the scattered helium ions the maximum loss of energy has been estimated on the base of superficial mass of gold foil and stopping power [11]. The results of the calculation and the measured energies of the helium ions are collected in Table 6. The calibration made with the PAC source has been used. In Fig. 7 are presented the energy spectra of helium ions  ${}^4_2\text{He}^+$  scattered on the gold foil of  $100 \mu\text{g}/\text{cm}^2$  recorded with the diamond detector. The silicon detector has been used for monitoring the operation of the accelerator.

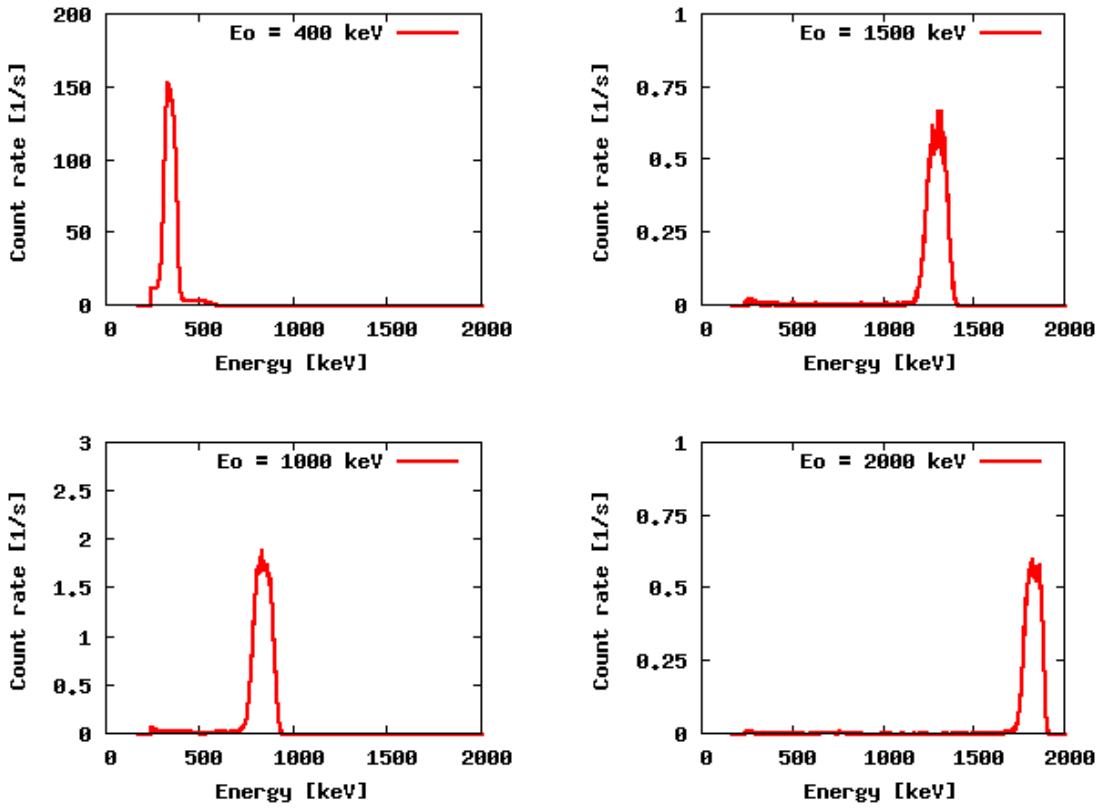


**Fig. 7.** Energy spectra of helium ions  $^{4}_{2}\text{He}^{+}$  scattered on gold foil of  $100 \mu\text{g}/\text{cm}^2$  recorded with the diamond detector.

**Table 6.** Calculated ( $E_1$  and  $E_3$ ) and measured ( $E_m$ ) energies of the helium ions.

$E_0$ (keV)	$E_1$ (keV)	$\sigma(E_1)$ (keV)	$E_3$ (keV)	$\sigma(E_3)$ (keV)	$E_m$ (keV)	$\Delta E$ (keV)
400	373	11	324	44	330	50
1000	933	27	908	54	826	110
1500	1399	40	1411	52	1350	130
2000	1866	54	1917	48	1836	96

Linearity of the amplitude signal has been investigated. In Fig. 8, the measured peak energy values  $E_m$  are plotted in function of the known values of the scattered helium ion energy  $E_1$  and peak positions  $E_t$  of the PAC source. All the points lie perfectly on the same calibration line, which is obtained from measurements with the monoenergetic beams only.

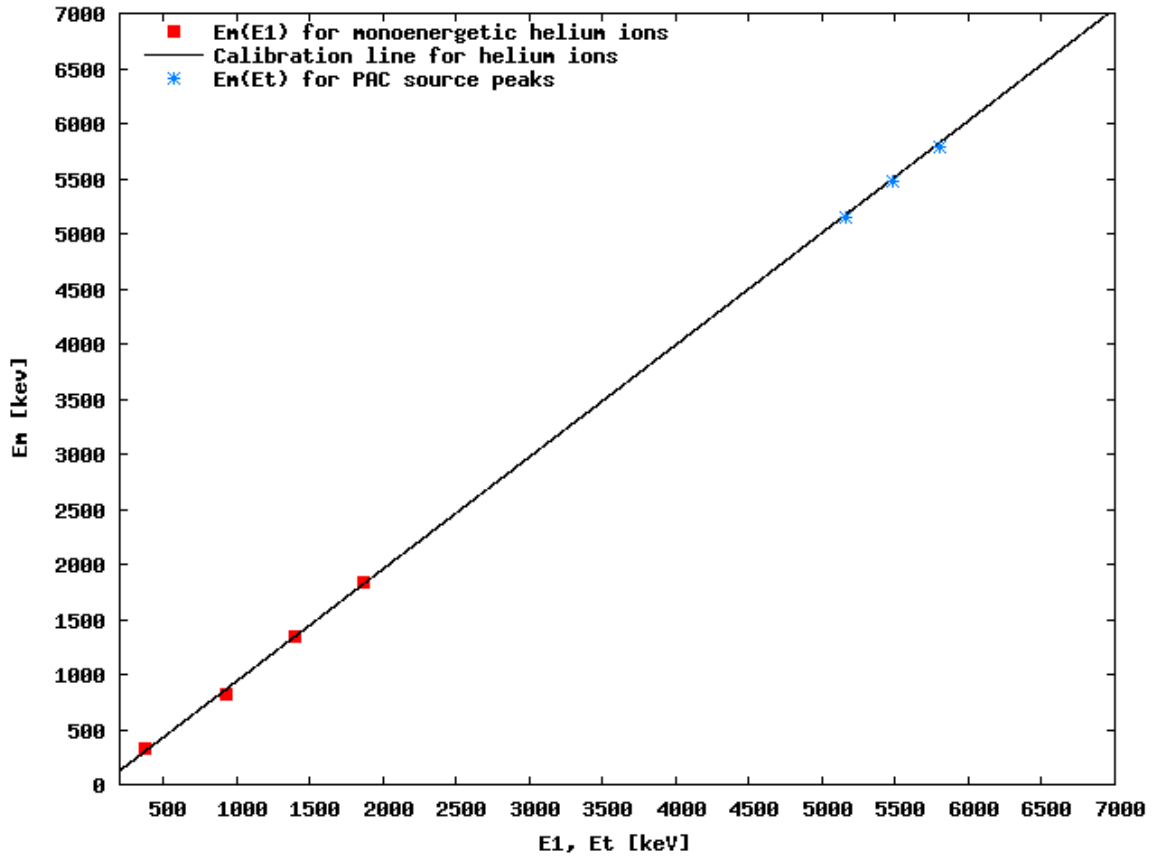


**Fig. 8.** Measured  $E_m$  vs reference (beam  $E_1$  or source  $E_t$ )  $\alpha$  energy.

#### 4. Conclusions

The experiment that has been carried out has been introductory for measuring spectrometric properties of the diamond detector used for the  $\alpha$  spectrometry. A very good energy resolution has been observed, comparable with the silicon detector resolution. The measured energy of the helium ions differs slightly from their calculated or estimated energy. However, the differences are on the order of the peak half-width only. From the performed experiment it is difficult to judge which reason of the broadening of peaks is. It can be at least partly generated by small differences in the energy of scattered ions.

The observed linearity of the energy measurements in the range investigated (0.4 to 2 MeV and extended to 5.8 MeV) is a very important property of the diamond detector. Future measurements of the lost alphas energy below 3.5 MeV at tokamaks will be significant for the thermonuclear plasma diagnostic.

More careful test experiments are expected in order to find out which factors influence results of the measurements for pure  $\alpha$  beams and with presence of other radiation ( $\gamma, n, t, d$ ) expected in a real surrounding of tokamaks.

## Acknowledgements

We are indebted to Prof. Marian Jaskoła and Dr. Andrzej Korman for preparation of the experiment at the Van de Graaff accelerator in the Soltan Institute of Nuclear Studies (Warsaw, Poland) and for their assistance at the measurements.

Special thanks are to Eng. Roman Hajduk and Mr. Władysław Janik from our Institute for their electronical and mechanical services.

## References

- [1] R. Aymar: ITER R&D: Executive summary design overview. *Fusion Eng. Design* **55** (2001) 107–118
- [2] G.J. Schmid, J.A. Koch, R.A. Lerche: A neutron sensor based on single crystal CVD diamond. *Nucl. Instrum. Meth. A* **527** (2004) 554–561.
- [3] C. Llewellyn Smith: The path to fusion power. *Eur. Phys. J. Special Topics* **176** (2009) 167–178.
- [4] D.S. Darrow , S.J. Zweben, H.W. Herrmann: Alpha particle loss diagnostics in TFTR and tokamak reactors. *Fusion Eng. Design* **34-35** (1997) 53-58.
- [5] M. Angelone, D. Lattanzi, M. Pillon. Development of single crystal diamond neutron detectors and test at JET tokamak. *Nucl. Instrum. Meth. A* **595** (2008) 616–622.
- [6] A. Galbiati, S. Lynn, K. Oliver: Performance of monocrystalline diamond radiation detectors fabricated using TiW, Cr/Au and a novel ohmic DLC/Pt/Au electrical contact. *IEEE Trans. Nucl. Sci.* **56** (2009) 1863–1874.
- [7] F. Foulona, P. Bergonzoa, V.N. Amosovb: Characterisation of CVD diamond detectors used for fast neutron flux monitoring. *Nucl. Instrum. Meth. A* **476** (2002) 495–499.
- [8] A. Mainwood: CVD diamond particle detectors. *Diamond Rel. Mater.* **7** (1998) 504-509.
- [9] F. Nava et. al.: Transport properties of natural diamond used as nuclear particle detector for a wide temperature range. *IEEE Trans. Nucl. Sci.* **26** (1979) 308–315.
- [10] [www.slac.stanford.edu](http://www.slac.stanford.edu) Diamond detectors with subnanosecond time resolution for heavy ion spill diagnostics.
- [11] NUCLEONICA – a new nuclear science web portal from the European Commission’s Joint Research Centre containing the compiled base of data. <http://www.nucleonica.net> .
- [12] F. Bassani, G. L. Lield, P. Wyder: Encyclopedia of Condensed Matter Physics. Elsevier Ltd, 2005.